PANAMGEO CHILE 2024
17th PAN-AMERICAN CONFERENCE ON SOIL MECHANICS AND GEOTECHNICAL ENGINEERING | 2nd LATIN-AMERICAN REGIONAL CONFERENCE OF IAEG
LA SERENA • CHILE / NOVEMBER 12 - 16, 2024

Proceedings of the 17th Pan-American Conference on Soil Mechanics and Geotechnical Engineering (XVII PCSMGE), and 2nd Latin-American Regional Conference of the International Association for Engineering Geology and the Environment (IAEG), La Serena Chile, 2024.

Coupled analysis of dynamic soil-structure interaction of masonry buildings founded on fissured clayey soil

Análisis acoplado de la interacción dinámica suelo-estructura de edificaciones de mampostería cimentadas en suelo arcilloso agrietado

Sergio Martínez-Galván,
Geotecnia, Sección de Estudios de Posgrado e Investigación, Escuela Superior de Ingeniería y Arquitectura Zacatenco, Instituto Politécnico Nacional, México, samartinezg@ipn.mx

Gabriel Auvinet, Moisés Juárez and Edgar Méndez
Geotecnia, Instituto de Ingeniería, Universidad Nacional Autónoma de México, México

ABSTRACT: The purpose of this article is to show that a house's structure and foundation built on a fissured supporting soil can suffer severe damage due to local seismic amplification. The study refers to a two-story masonry house typical of those found in many areas of Mexico City founded on a slab. The analysis includes the review of the foundation for the limit states of failure and serviceability. The foundation load capacity is estimated both by a conventional analysis and by an alternative method based on the characteristic planes technique. The settlement analysis considers the service load, the presence of fissures in the ground surface and regional subsidence. The house seismic response evaluation includes vertical and horizontal forces and overturning moment. The analysis of the foundation settlements and of the house seismic response is performed with a 3D finite element model that includes the stratigraphy, the fissured soil on the surface, as well as the foundation and structure of the house. The fissures are modeled with soil-soil interfaces. The site stratigraphy includes a clay formation of considerable thickness and a vertical basalt flow step at depth, such as that detected in the municipalities of Iztapalapa and Tláhuac, Mexico City. The seismic response analysis indicates that in this special condition there is a substantial amplification with respect to the response spectrum normally expected at the site where the house is located.

KEYWORDS: fissured clayey soil, dynamic soil-foundation-structure interaction, analysis 3D, finite element, masonry house

1 INTRODUCTION

This article illustrates the local seismic amplification that can occur in a two-story masonry house with irregular height in an area with fissures in the ground surface like those observed in Iztapalapa and Tláhuac municipalities, Mexico City.

1.1 *Background*

Auvinet, 2010, Méndez *et al*. 2012 and Auvinet *et al*. 2013, 2015, 2017, 2019, 2020, 2021 document and investigate the crack generation mechanisms observed on the ground surface in the southwest of Mexico City. They indicate that the fissures generation mechanism is a consequence of the differential regional subsidence due to exploitation of water from deep aquifers in combination with the variable thickness of the clay formation.

The house foundations affectation by differential subsidence generated by regional consolidation is more severe when there is a basalt flow step at depth. These houses are more prone to collapse when a severe earthquake occurs.

Martínez-Galván *et al*. 2021 presents a seismic amplification analysis in an area with surface cracking during the earthquake of September 19, 2017.

1.2 *Aim and scopes*

The article's aim is to show that in special conditions such as fissuring of the ground houses that have been considered as safe by technical inspection can suffer serious damage to their structure and foundation due to a severe earthquake. The analysis methodology presented here complements the foundation vulnerability evaluation presented by Velasco *et al*. (2022).

Scopes:

a) Calculation of foundation ultimate load capacity and stability evaluation for load combinations. This calculation considers analytical methods and an alternative procedure based on combined load envelopes known as characteristics planes, Gourvenec (2007), Salençon and Pecker (1995-a, 1995-b).

b) Review of the failure and serviceability limit states of the foundation in accordance with local regulations (GCDMX, 2017c).

c) House seismic response calculation with a 3D finite element model in time domain, with Plaxis 3D software, Plaxis bv 2020. This analysis considers the foundation settlement calculation due to service load and regional consolidation. The seismic response calculation is in terms of the maximum acceleration for an equivalent earthquake (intraplate), like the seismic event that occurred on September 19, 2017, with magnitude 7.1. In the seismic response analysis, the soil behavior is considered as undrained with parameters defined from the shear wave velocity profile and Poisson's ratio of 0.495.

2 INPUT DATA

2.1 *Study site*

The study site is at Colonia Del Mar, in the lake zone, Tláhuac municipality. This site is representative of the land superficial cracking that occurs in the Mexico City southeast.

2.2 *The soil*

Through deep geotechnical exploration carried out in 2019 in this area (Auvinet *et al*. 2021), the horizontal variability of clay formation thickness was confirmed. Based on this geotechnical exploration:

- The representative stratigraphic profile presents an abrupt change of 32 meters in the clay formation thickness, between two electrical cone penetration tests, CPTu-02 and CPTu-03, Figure 1. This abrupt change is a result of a vertical front generated by a basalt flow buried by the lacustrine clay formation.
- The stratigraphy is as follows:

a) Superficial crust or anthropic landfill, made up of sandy silt or silty sand that present cohesion, with variable thickness of 2.0 to 3.0 meters.

b) Clay formation with sand lenses intercalations of 0.10 to 0.30 meters of thick. Total thickness of the clay formation varies from 56.0 to 90.0 meters.

c1) Under the clay in the CPTu-03 located to east, at a depth of 56 meters, sandy silt or compact silty sand (defined as deep deposits) with a thickness of 9.40 m.

c2) Under the clay in the CPTu-03 located to west, at a depth of 90 meters with an explored thickness of 10.2 meters, deep deposits are found.

d) Fractured basalt.

- Figure 1 shows the shear wave velocity profile (*Vs*), determined by suspended probe tests carried out in the CPTu-2 well. The *Vs* magnitude varies from 40 m/s in the upper clay formation to 150 m/s in the deep deposits of silty sandy. The average *Vs* weighted by the thicknesses considered, in 80 meters of soil tested, is 87.1 m/s. The undrained rigidity modulus calculated with the shear wave profile allows calculating the surface response and comparing the maximum acceleration with response spectra of the cracked area and of the free field zone without crack.
- Figure 2 shows the pore pressure profiles determined with piezocone tests at the CPTu-2 and CPTu-3 wells. In June 2019, the pore pressure was hydrostatic up to 30 meters deep and, at greater depths, a reduction of pore pressure was observed due to the exploitation of deep aquifer. The groundwater level (NAF) is at a depth of 2.7 m.
- Table 1 shows the mechanical drained parameters of the soil strata A, crust and B, clay formation, used in the calculation of soil settlement, parameters of the hardening soil model. Clay formation parameters correspond to one-dimensional consolidation tests and drained resistance parameters correspond to correlations based at Alberro and Hiriart (1973). For unit A, crust, the resistance and deformation parameters correspond to average values of triaxial tests, CU-type. Table 1 shows elastic deformation parameters of units C y D, obtained with correlations from the material classification, Bowles (1997).

2.3 *House structure and loads*

Structure features, Figure 3:

- A two-level house with reduction in built area on the second level compared to the ground floor. The ground floor is 8.0x12.0m. The reduction is only in the short direction, from 8.0 to 5.0 meters built, i.e. 37.5% less. From the point of view of vulnerability analysis, this change in height causes this house to be classified as very irregular (Velasco *et al*. 2022).
- Structural elements dimensions: height of each level is 2.7 m. The walls are 12 cm thick and are made up of clay blocks, 15x15 cm columns and 15x20 cm beams. The thicknesses of the roof, first level and foundation slabs are respectively 6, 8 and 12 cm.
- The columns, beams and slabs are made of reinforced concrete, and the house was self-built. Figure 3 shows the distribution of masonry walls and columns. The foundation slab covers the plan area of 8x12 m.

a) Plan view, location of borings, Colonia Del Mar site,

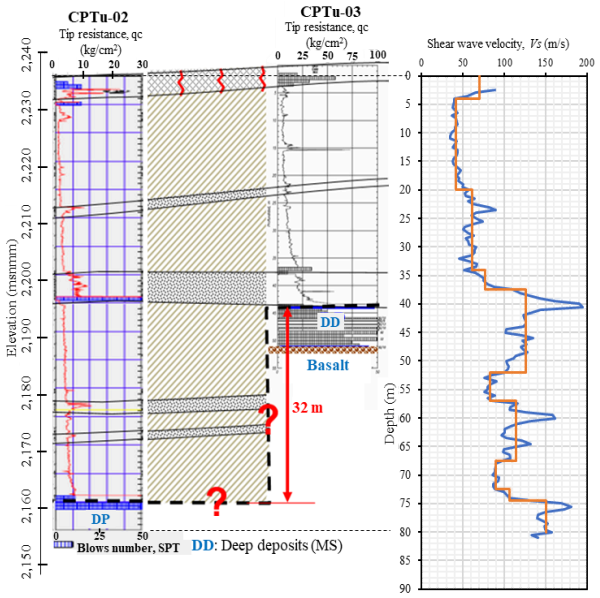

b) Cross section, Colonia Del Mar site

Figure 1. Stratigraphic profile at the study site, modified from Auvinet *et al*. 2021.

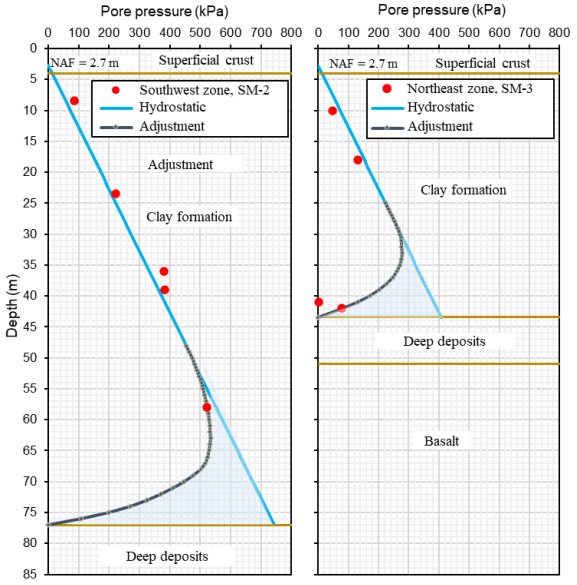

Figure 2. Pore pressure profiles determined at the CPTu-2 and CPTu-3 borehole sites, modified from Auvinet *et al*. 2019.

Table 1. Resistance, deformation, and compressibility parameters of the soil strata used in the analysis.

Parameter \ Unit	A. Crust	B. Clay formation			C. Deep deposits	D. Basalt
Depth (m), zone with greater clay thickness	0.0 – 4.0	4.0 – 35.0	35.0 – 43.4	43.4 – 77.0	77.0 – 80.0	---
Depth (m), zone with smaller clay thickness	0.0 – 4.0	4.0 – 35.0	35.0 – 41.0	---	41.0 – 51.0	51.0 - 80.0
Volumetric weight, γ_s (kN/m^3)	14.0	12.0	12.0	12.0	20.0	22.0
Undrained cohesion, c_u (kPa)	26.0	14.0 – 32.0	35.0 – 45.0	---	---	---
Cohesion, c' (kPa)	30.0	1.0	1.0	1.0	---	---
Internal friction angle, φ' (grades)	30.0	30.0	30.0	35.0	---	---
Tension cut off, R_T (kPa)	1.0	1.0	1.0	1.0	---	---
Deformation module, E' (kPa)	12,000	---	---	---	50,000	5.0E+6
Poisson ratio, υ (---)	0.30	0.30	0.30	0.30	0.30	0.20
Void ratio, e_0 (---)	---	9.0	7.0	4.5	---	---
Compression index, C_c (---)	---	9.33	5.52	5.34	---	---
Recompression index, C_s (---)	---	1.87	1.10	1.07	---	---
Overconsolidation ratio, OCR (---)	---	1.10	1.20	1.20	---	---
Ground pressure at rest coefficient, K_0 (---)	0.43	0.54	0.54	0.54	0.43	0.25

- The structural elements behavior model is linear elastic. Table 2 shows the elastic parameters used in the analysis.
- Table 3 shows the resulting forces for the load combinations (vertical force, V, horizontal force, H, overturning moment, M) used in the geotechnical revision of the foundation. H and M are in both orthogonal horizontal directions and them include static and seismic load.
- The load combinations and load factors (F_C) used in this study comply with the provisions of the NTC- on Criteria and Actions for the Structural Design of Buildings (NTC-CADEE, GCDMX, 2017a). The seismic loads include the recommendations of NTC-for Earthquake Design (NTC-DS, GCDMX, 2017d).
- The seismic load calculation includes:

$$\frac{c}{Q'R} = 0.326 \qquad (1)$$

this value corresponds to the plateau of the design spectrum shown in Figure 4 (SASID, 2017), where c is the seismic coefficient, Q' is a factor that depends on the reduction factor for seismic behavior, Q (=2, masonry) and R is the reduction factor due to over-resistance. The irregularity factor is = 0.8, due to the reduction of built area in the second level (NTC-DS, GCDMX, 2017d).
- Table 3 shows the resulting mechanical elements from load combinations of the two-story housing, the load factors and vertical force calculated by tributary area. Calculation of overturning moments and the basal shear forces are with pseudo-static method (NTC-DS, GCDMX, 2017b) and Eq. (1).

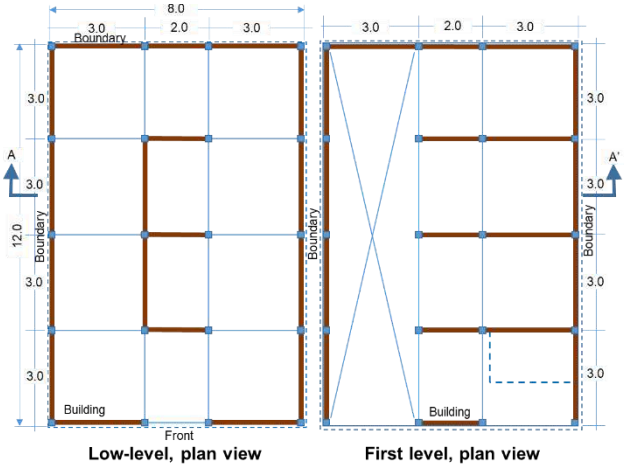

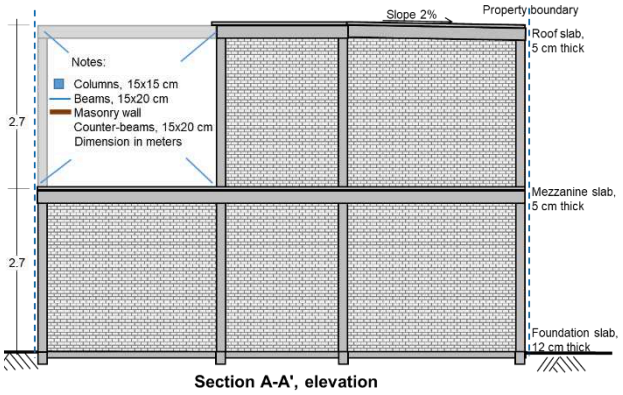

Figure 3. Structural elements distribution of the two-level housing.

Table 2. Elastic parameters of structural elements of the housing.

Element Parameter	Reinforced concrete (slabs, columns, beams)	Masonry wall
f´c (MPa)	25.0	---
E (kPa)	2.214E+07	7.000E+05
G (kPa)	9.223E+06	2.800E+05
υ (---)	0.20	0.12
Ed (kPa)	2.214E+07	1.200E+06
Gd (kPa)	9.223E+06	4.800E+05

Notes: *f´c*, unconfined compression strength, *E* and *G*, deformation and shear stiffness modules to sustained loading; *υ*, Poisson's ratio; *Ed* and *Gd*, deformation and shear stiffness modules to short-term loads. The parameters of the masonry wall defined on the recommendation of the NTC-DCEMC (GCDMX, 2020, p.51) for confined walls and reduction factor of 50% to consider self-construction and compressive strength of the wall, f^*m = 4.0 MPa.

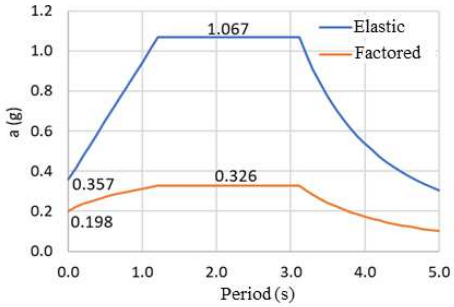

Figure 4. Design spectrum of the study site (SASID, 2017).

Table 3. Resulting from load combinations, two-story housing.

Load combination	V kN	H_T kN	H_L kN	M_T kNm	M_L kNm	|H| kN	|M| kNm
1. 1.3CM+1.5CVm	2261.4	0.0	0.0	582.3	179.2	0.0	609.3
2. 1.1(CM+CVa+1.0Sx+0.3Sy)	1636.8	533.6	160.1	2426.8	718.9	557.1	2531.1
3. 1.1(CM+CVa+1.0Sx+0.3Sy)	1636.8	533.6	-160.1	2426.8	-210.1	557.1	2435.9
4. 1.1(CM+CVa+1.0Sx+0.3Sy)	1636.8	-533.6	160.1	-609.2	718.9	557.1	942.3
5. 1.1(CM+CVa+1.0Sx+0.3Sy)	1636.8	-533.6	-160.1	-609.2	-210.1	557.1	644.4
6. 1.1(CM+CVa+1.0Sx+0.3Sy)	1636.8	160.1	533.6	1364.2	1802.9	557.1	2260.9
7. 1.1(CM+CVa+1.0Sx+0.3Sy)	1636.8	160.1	-533.6	1364.2	-1294.1	557.1	1880.4
8. 1.1(CM+CVa+1.0Sx+0.3Sy)	1636.8	-160.1	533.6	453.4	1802.9	557.1	1859.0
9. 1.1(CM+CVa+1.0Sx+0.3Sy)	1636.8	-160.1	-533.6	453.4	-1294.1	557.1	1371.2
10. 1.0(CM+CV)	1417.4	0.0	0.0	0.0	111.9	0.0	381.4

Notes: vertical force (*V*), transversal and longitudinal basal shear forces (H_T, H_L), transversal and longitudinal turning moments (M_T, M_L), basal shear force module (|*H*|), turning moment module (|M|). Dead load (*CM*); accidental, maximum, and average live load (*CVa*, *CVm*, *CV*), transverse and longitudinal seismic forces (*Sx*, *Sy*). Transversal and longitudinal are relative to foundation dimensions. Shear forces and moments include static and seismic loading.

2.4 *Seismic environment*

The calculation of the uniform hazard spectrum (UHS) of the study site for a return period of 475 years and the corresponding synthetic earthquake are with the Prodisis program (CFE, 2015), Figure 5.

As reference, to calibrate the free-field surface response of the analysis model, defined as the response in the area far from the influence of the basalt front, the maximum accelerations measured in areas close to the study site are considered. Table 4 shows the summary of the maximum accelerations of seismic measurement stations close to the study site. Extreme maximum acceleration corresponds to station XO36 located in Xochimilco, lake zone. Figure 6 shows the location of the seismic measurement stations and the study site (partially transparent red circle).

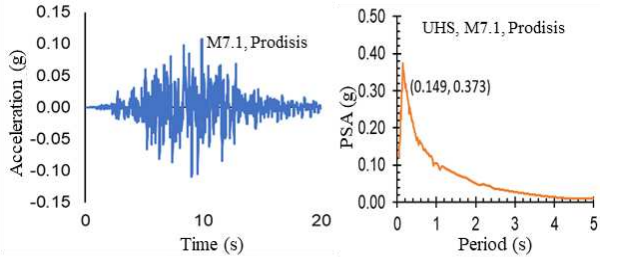

Figure 5. Uniform hazard spectrum (UHS) for an intraplate earthquake of intermediate depth and for a return period of 475 years. Source: Prodisis (CFE, 2015).

Table 4. Summary of maximum accelerations measured on the surface, source: http://www.cires.org.mx/ .

Id	Location	Amax (g)
FJ74	Javier Barros Sierra Foundation, (Lake zone)	0.092
TP13	Elementary School "May 1st.", Tlalpan, (Lake zone)	0.067
GC38	Kindergarten "Luz G. Campillo", (Transition zone)	0.126
CU80	Elementary School "R. López Velarde", (Lake zone)	0.168
XO36	Kindergarten "Xochimilco Club España y Chicoco", (Lake zone)	0.174

Note: Amax, maximum acceleration on the ground surface.

3 EVALUATION OF FAILURE LIMIT STATE

3.1 *Loading capacity*

The ultimate vertical force (V_u) is:

$$V_u = q_u A_c \tag{2}$$

where A_c, is plan area of the foundation and q_u, the ultimate load capacity of the foundation which, for a surface slab, the calculation is with:

$$q_u = c_u N_c s_c d_c + q_0$$

$$s_c = 1 + 0.2B/L \;;\; d_c = 1 + 0.27\sqrt{D/B} \tag{3}$$

$$q_0 = \gamma D_f$$

where $c_u (= 22.6\, kPa)$, undrained cohesion determined in non-consolidated non-drained triaxial test (Tx-UU); s_c, form factor; $N_c (= 5.14)$, cohesive load capacity factor; d_c, depth factor; q_0, overload pressure adjacent to the foundation at the

foundation depth; B, L and D_f, width, length and depth of foundation, respectively; γ, volumetric weight of the soil adjacent to the foundation. Undrained cohesion (c_u) is weighted by the thickness of the soil strata that range from the surface to a depth of 0.7B (=5.6 m), Table 1.

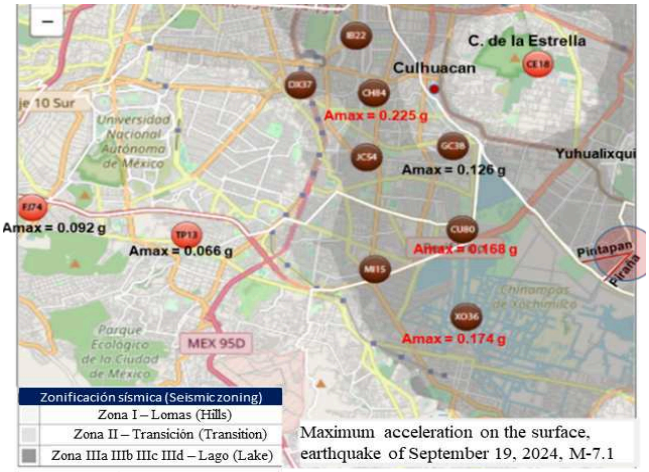

Figure 6. Maximum accelerations measured on the surface; earthquake of September 19, 2017. Modified from: http://www.cires.org.mx/ .

The ultimate horizontal force (H_u) and ultimate overturning moment(M_u)of a foundation slab are calculated with (Gourvenec, 2007):

$$H_u = c_u A_c \tag{4}$$

$$M_u = c_u N_{cM} A_c B \tag{5}$$

$$N_{cM} = 0.64 + 0.05 B/L \tag{6}$$

Based on the geometry of the foundation slab and the undrained cohesion of the shallow soil strata, the ultimate resisting forces and moments are:

V_u = 12,626.6 kN (12.63 MN)

H_u = 2,166.9 kN (2.17 MN)

M_u = 11,672.1 kN-m (11.67 MN-m)

The resistance factors (F_R) that apply to this study, F_R = 0.65 (NTC-DCC, GCDMX, 2017-c) and the factored resisting forces and moments are:

V_F = 8,207.3 kN (8.21 MN)

H_F = 1,408.5 kN (1.41 MN)

M_F = 7,586.9 kN-m (7.59 MN-m)

with F_R = 0.35, optional:

V_F = 4,419.3 kN (4.42 MN)

H_F = 758.4 kN (0.76 MN)

M_F = 4,085.2 kN-m (4.09 MN-m)

3.2 *Failure limit state review, characteristic plans*

An alternative way to evaluate the failure limit state of a foundation is through the concept of characteristic planes. These planes define failure envelopes. Admissible load envelopes consider reduction factor.

Gourvenec (2007) indicates that rectangular foundations failure mechanism under combined general loading presents great similarity to failure in plane strain and depends on the shape factor (s_c). This ultimate limit state can be calculated from a standard envelope with the magnitude of the ultimate loads: V_u, H_u, M_u of the specific analysis case. Figure 7 shows failure envelopes with unitary normalized load. For the studied case, the relations to generate the envelopes are:

- plane V_N - H_N ($V_N = V/V_u$, $H_N = H/H_u$ and M=0)

$$V_N = 0.5 + 0.5\sqrt{1 - H_N}\,;\ H_N = 1 \text{ para } V_N \leq 0.5 \tag{7}$$

- plane V_N - M_N ($V_N = V/V_u$, $M_N = M/M_u$ and H=0)

$$M_N = 4\left(V_N - V_N^2\right) \tag{8}$$

- plane H_N - M_N ($H_N = H/H_u$, $M_N = M/M_u$ and V is variable)

$$\left(\frac{H_N}{H_N^*}\right)^2 + \left(\frac{M_N}{M_N^*}\right)^2 = 1 \tag{9}$$

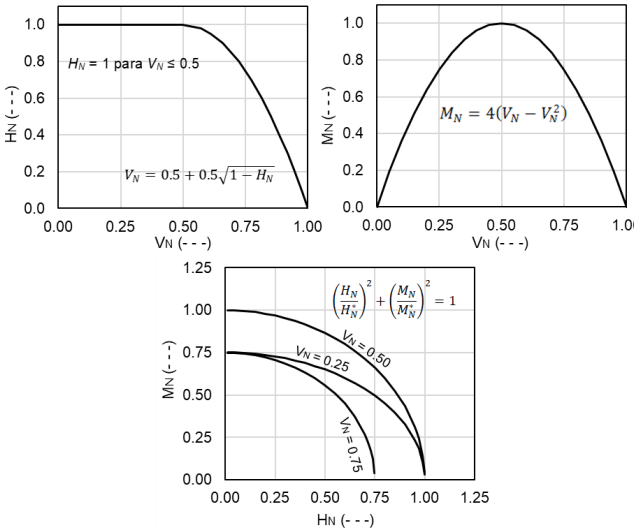

Figure 7. Envelopes of normalized (unitary) ultimate loads, modified from Gourvenec (2007).

Calculation of the factored loads envelopes (V_F, H_F, M_F):

a) Ultimate envelopes generation, Figure 8: multiplying unitary ultimate envelopes points by the ultimate loadsV_u, H_u, M_u calculated with Eqs 7, 8, 9. These graphs show the failure limit state of the house foundation in review.

b) Factored envelopes generating, Figure 8: multiplication of ultimate envelopes points by factored load, section 3.1.

Based on the resulting loads of the two-story house (Table 3), for each resistance factor (F_R) considered and for each load combinations considered, the ratio V/V_u results, Table 5. The evaluating of the failure limit states and, each characteristic plan (Figure 8) is for the combination 1, static load and for combinations 2 to 9, seismic load.

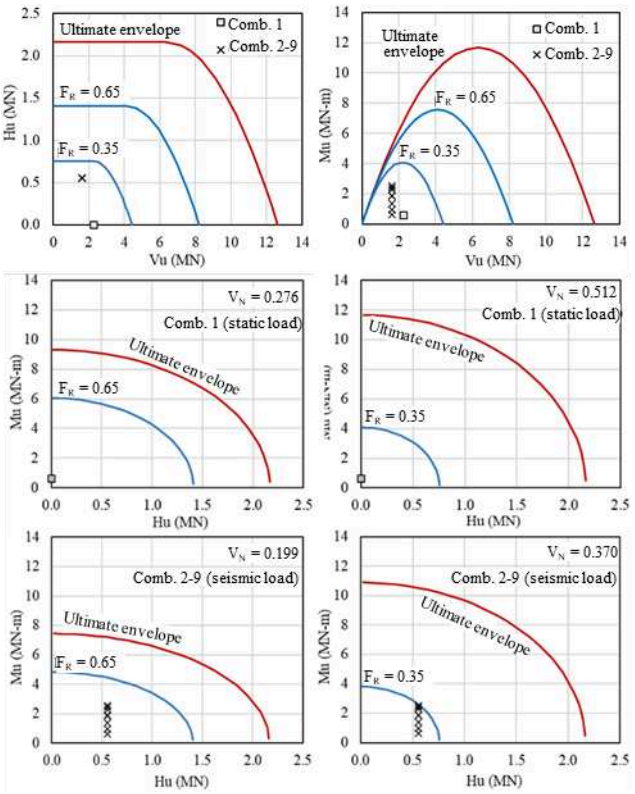

Figure 8. Envelopes of ultimate loads and factored loads, of the case under review, two-level housing.

Table 5. $V_N = V/V_u$ ratios resulting from the load combinations of the two-story house.

Load combination	F_R=0.65 V/V_u (---)	F_R=0.35 V/V_u (---)
1	0.276	0.512
2 a 9	0.199	0.370
10	0.173	0.321

Note: F_R, resistance factor; V, vertical force; V_u, ultimate vertical force.

3.3 *Review of the limit state of failure, local regulations*

The NTC-DCC (GCDMX, 2017-b) indicates that for superficial foundations compliance with the following inequality will be verified for the different possible combinations of vertical actions:

$$\frac{\Sigma QF_C}{A} < r \tag{10}$$

where: $\sum QF_C$ is the sum of the vertical actions to be taken into account in the combination considered at planting depth, affected by their respective load factor, F_C; A is the area of the foundation element; r is the reduced unit load capacity of the foundation (*i.e.* affected by the corresponding resistance factor, F_R).

For foundations on cohesive soils:

$$r = \left[c_u N_c\right] F_R + p_v \tag{11}$$

where: c_u is the undrained cohesion; p_v is the total vertical pressure at planting depth due to the soil own weight; N_c is:

$$N_c = 5.14\left(1 + 0.25D_f/L + 0.25B/L\right) \tag{12}$$

for $D_f/B < 2$ and $B/L < 1$, where B, L, D_f already defined.

If D_f/B and B/L do not comply with the previous inequalities, these relations will be considered equal to 2 and 1, respectively.

When considering the geometry of the foundation slab and the value of undrained cohesion (22.6 kPa):

$D_f/B = 0.0 < 2$ and $B/L = 0.667 < 1$, therefore
$N_c = 5.14(1 + 0 + 0.25(8/12)) = 5.997$
$r = [(22.6)(5.997)]0.65 + 0.0 = 88.10$ kPa
$r = [(22.6)(5.997)]0.35 + 0.0 = 47.44$ kPa

Table 6 shows the mean pressure (p_m) calculated with:

$$p_m = V/A_C \tag{13}$$

The calculation of load eccentricities in both horizontal directions (e_T and e_L, respectively) is with (Table 6):

$$e_T = M_T/V\ ,\ e_L = M_L/V \tag{14}$$

The calculation of pressure increases per overturning moment generated by static and seismic actions ($\pm\Delta p_{eT}$, $\pm\Delta p_{eL}$) is with (Table 6):

$$\pm\Delta p_{eT} = (M_T B/2)/I_T\ ,\ \pm\Delta p_{eL} = (M_L L/2)/I_L \tag{15}$$

where I_T, I_L are the transverse and longitudinal foundation inertia moments, respectively, and the overturning moments M_T, M_L correspond to static or seismic load. The maximum and minimum accumulate pressures $\left(p_{Tmax}, p_{Tmin}, p_{Lmax}, p_{Lmin}\right)$ include the effect of the static overturning moment and seismic load.

The verification of the inequality of Eq. 10, where the compression pressures do not exceed the reduced unit load capacity (r) for the F_R considered, so the foundation a compression load is adequate, Table 6. However, in combinations 2 and 3 tensions or tractions appear with very low values, 1.9 kPa. The vertical irregularity of the structure and seismic load causes tensions in the foundation. In this case, the calculation of the overturning moments is based on the gravitational forces calculated in turn by tributary area, so the overturning moments thus calculated do not include the rigidity of the structural elements and the load-bearing walls. Due to the above, it is possible that tension will not be generated in the soil.

Table 6. Average pressure and pressure increment of the load combinations of the two-level house.

Variable	Combination									
	1	2	3	4	5	6	7	8	9	10
p_m, kPa	23.56	17.05	17.05	17.05	17.05	17.05	17.05	17.05	17.05	14.76
e_T, m	0.258	1.483	1.483	-0.372	-0.372	0.833	0.833	0.277	0.277	0.257
e_L, m	0.079	0.439	-0.128	0.439	-0.128	1.101	-0.791	1.101	-0.791	0.079
$\pm\Delta p_{eT}$, kPa	4.5	19.0	19.0	4.8	4.8	10.7	10.7	3.5	3.5	2.8
$\pm\Delta p_{eL}$, kPa	0.9	3.7	1.1	3.7	1.1	9.4	6.7	9.4	6.7	0.6
p_{Tmax}, kPa	28.11	36.01	36.01	21.81	21.81	27.71	27.71	20.59	20.59	17.61

p_{Tmin}, kPa	19.01	-1.91	-1.91	12.29	12.29	6.39	6.39	13.51	13.51	11.92
p_{Lmax}, kPa	24.49	20.79	18.14	20.79	18.14	26.44	23.79	26.44	23.79	15.35
p_{Lmin}, kPa	22.62	13.31	15.96	13.31	15.96	7.66	10.31	7.66	10.31	14.18
τ=88.10 kPa	ok	ok	ok	ok	ok	ok	ok	ok	ok	ok
τ=47.44 kPa	ok	ok	ok	ok	ok	ok	ok	ok	ok	ok

Note: negative indicates tension.

4 EVALUATION OF SERVICE LIMIT STATE

4.1 *Calculation of foundation settlement*

Settlement generated by the compressibility of the subsoil under the foundation is calculated with a 3D finite element numerical model (Plaxis bv., 2020), for the service load of the structure and its foundation and by regional consolidation.

The behavior model of the clay formation is elasto-plastic with strain hardening criterion (hardening soil), that of the surface crust is elasto-plastic with Mohr-Coulomb failure criterion and that of the deep deposits and basalt, is linear elastic. Table 1 shows the parameters used in the analysis. The behavior model of the structural elements of the house and its foundation is linear elastic. Table 2 shows the parameters of the structural elements. In the case of walls, the parameters correspond to sustained load.

The applied service load (combination 10, Table 6) is trapezoidal, in the foundation short direction with maximum and minimum magnitudes of 17.6 and 11.9 kPa, respectively, and, in the long direction, of 15.4 and 14.2 kPa, respectively.

Figure 9 shows that the settlement generated by the service load is not uniform in the foundation slab. The calculated maximum settlement of 27.5 cm is in the semi-width of the slab on the side with the most load and the minimum, 25.7 cm, in the corners of the side with the least load. The average total settlement is not adequate according to what is indicated in NTC-DCC (GCDMX, 2017b, p.17), because it exceeds the permissible value of 15 cm. However, if the house that make up a block retain a maximum of two levels of construction, this helps the settlement to be quasi-uniform in the reference block.

The angular distortion calculated in the foundation from Figure 9b is 0.00252 m/m, less than the acceptable inclination of (100/(100+3hc)) % = 0.00854, where hc= house height = 5.4 m, in accordance with the NTC-DCC (GCDMX, 2017b, Table 3.1.1).

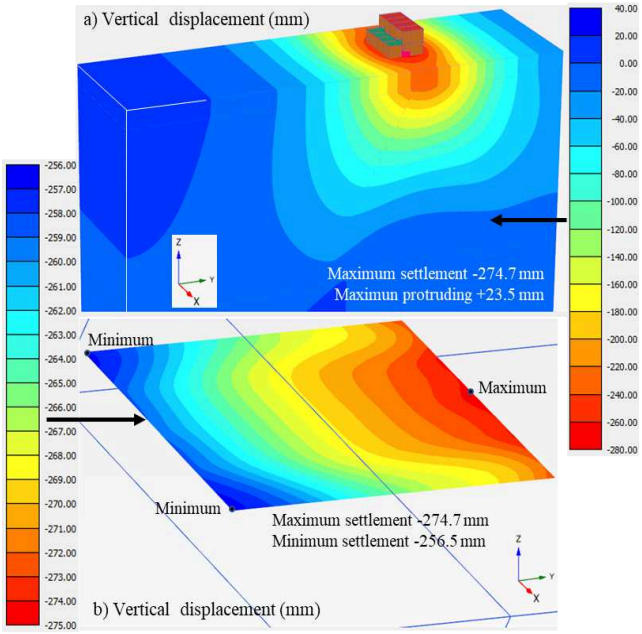

Figure 9. Calculated consolidation settlement for service load, combination 10, Table 6.

Figure 10 shows that the limit pressure is 21.95 kPa. The limit pressure is what generates the limit differential distortion. The calculation of the differential distortion is with the settlements calculated at the points indicated in Figure 9 for various load increments. The limit pressure is close to the average service pressure of combination 10 (14.76 kPa, Table 6), as shown by the ratio: 21.95/14.76 = 1.49. For a third level in the house, the limit differential distortion is reached.

The curve in Figure 10 is characteristic of the service load of the two-story house with a foundation slab supported on the stratigraphy indicated in Figure 1 and characterized with the parameters indicated in Table 1.

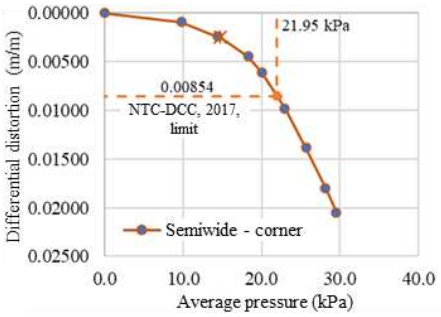

Figure 10. Limit pressure of the foundation slab of the two-story house for permissible deformation.

Figure 11-a shows that the settlement generated by regional consolidation is not uniform and Figure 11-b shows that the differential in the foundation slab is 31.5 cm and in the opposite direction to that calculated by the service load. The rigidity of the foundation slab causes the differential settlement trend to be linear and, in addition, the configuration shown in Figure 9-b is lost.

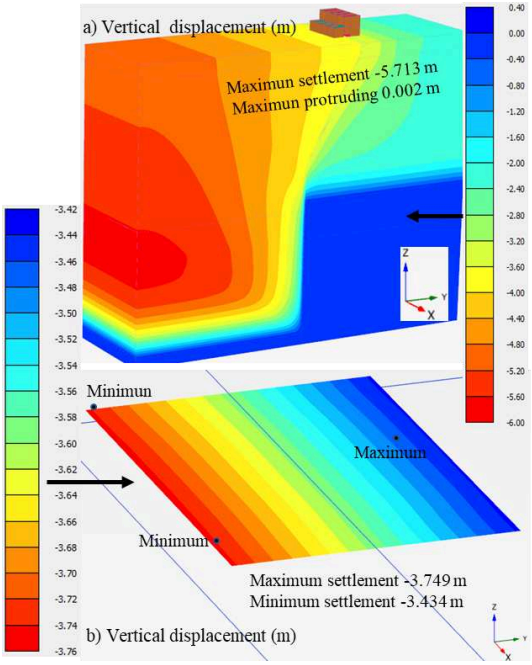

Figure 11. Settlement due to regional consolidation accumulated to those generated by service load (combination 10, Table 6).

If the second level occupies the other side of the property, the settlement by service load and by regional consolidation would cause the foundation rotation and the structure collapse. The presence of the buried basalt front and the crack on the surface, plus the development of regional consolidation generates settlements and lateral displacements at shallow depths that affect the house located near the crack trace.

5 SOIL-STRUCTURE SEISMIC RESPONSE

5.1 *Calculation of the structure natural period*

The calculate of the structural predominant period of the house structuring, Figure 3, is with a 3D finite element model (Plaxis bv., 2020), with the step-by-step dynamic procedure. The model considers the soil located from the surface and up to 29 m deep, Table 1, and includes masonry walls, beams, columns and roof, mezzanine, and foundation slab.

The analysis procedure considers a) application of horizontal forces of 30.0 kN at the intermediate intersections (column-beam) and 15.0 kN at the corner intersections, this at the roof level on the right side, Figure 3. b) In a second analysis stage, cancellation of these horizontal forces and the structure vibrates freely, dynamic procedure in time domain. The dynamic time of evaluating are 0.35 seconds.

Figure 12 shows the acceleration calculated in the roof slab and the corresponding response spectrum, where the predominant period is 0.05s (or frequency of 20 Hz).

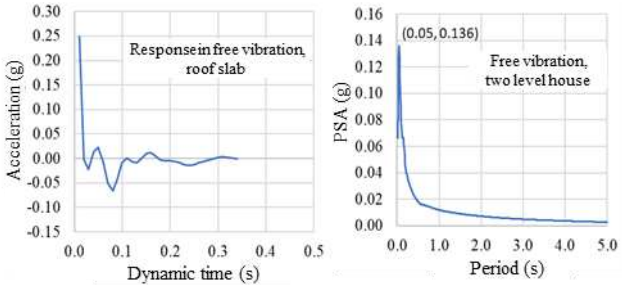

Figure 12. Response to roof slab vibration of the house.

5.2 *Calculation of the soil seismic response*

The calculating of the surface response of the study site and its respective dominant period for a seismic equivalent to the earthquake of September 19, 2017, is with a 3D finite element model (Plaxis bv., 2020), at time domain. The model considers the soil located from the surface and up to 80 m deep, Table 1, a vertical basalt front at depth and the shear wave velocity profile, Figure 3. The numerical model includes absorbing limits on the vertical sides to avoid the reflection of shear waves.

In the study site crosses a surface crack like those observed in the municipalities of Iztapalapa and Tláhuac, Mexico City. The modeling of discontinuity generated by the surface crack is with soil-soil interface.

According to Martínez-Galván *et al*. (2021), for an earthquake equivalent to that of September 19, 2017 (Figure 5), the surface seismic response of the site leads to a maximum acceleration that varies between 0.24 - 0.26 g. Figure 12 shows the corresponding response spectrum. The dominant period at free field is 0.71 s.

5.3 Calculation of the soil-structure seismic response

The seismic response calculation of the house structure (Figure 3) and soil (stratigraphy and shear wave velocity profile of the soil, Figure 1) is with a 3D finite element model (Plaxis bv., 2020) with a dynamic procedure in the time domain. The model considers the soil located from the surface and up to 80 m deep, Figure 1. The earthquake applied at the base of the model is equivalent to the one that occurred on September 19, 2017, Figure 5. The numerical model includes absorbing limits on the vertical sides to avoid the reflection of shear waves. The modeling of discontinuity generated by the surface crack is with soil-soil interface.

The maximum acceleration calculated in the house roof is 0.620 g and in the first level, mezzanine, 0.576 g. Both magnitudes are greater than the value indicated on the plateau of the factored design spectrum of 0.326 g (Figure 4). Figure 13 shows the response spectrum calculated at the soil-slab contact, the maximum acceleration (ordered to the origin) is 0.41 g and the maximum amplification (PSA) is 1.32 g. The above shows that the frequency content of the September 19, 2017, earthquake and the site effects significantly increase the vibration of two-story masonry house affect by vertical irregularity (change in height) and by a surface crack.

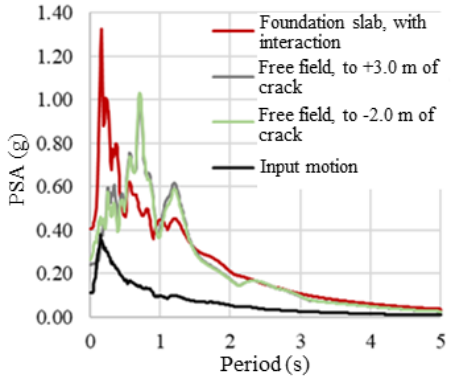

Figure 13. Free field response of the study site and the house foundation slab to an earthquake equivalent to September 19, 2017.

6 DISCUSSIONS

The great compressibility of the clay formation generates structural damage to the house and the foundation. A substantial increase in differential settlement is generated due to regional consolidation when the house is near or above a fissure. Photographic evidence of damage caused by cracking of the ground surface is indicated in *Background* (subcap. 1.1 of this paper), an example of the houses damage, Figure 14.

Figure 14-a shows the surface path of three cracks and the location of 16 houses damages. The fissures A and B show stepway that have generated the demolition of house 05 and damage of houses 07 and 09, Figure 14-b.

The deeply buried basalt (geological feature) generates local seismic amplification close to the cracking on the surface that complements the collapse of the house, like evidenced by the national newspapers after the earthquake of September 19, 2017.

7 CONCLUSIONS

The review of the failure limit state of the foundation slab of the considered house shows that the foundation is adequate in accordance with the NTC-DCC (2017b). For the optional case of considering $F_R = 0.35$, the proposed procedure of characteristic planes shows that there may be instability under load with earthquake effects.

The review of the service limit state of the foundation slab of the considered home shows that it is not adequate in accordance with the NTC-DCC (2017b), because the magnitude of the total settlement exceeds the permissible limit. The above could be mitigated if the structural house that make up a block kept two levels at most. For the vertical irregularity of house analyzed, the regional consolidation together with the presence of the basalt front in depth and the crack on the surface, counteract the differential settlement of the service load, the foundation desarrolles in contrary way differential settlement not permissibles. If the second level changes to the other side in the short side of the housing structure, the settlements in the foundation slab by service load would plus be due to regional consolidation and could cause collapse in a short period of house service.

The site effects, particularly the presence of the basalt front at depth, substantially increase the seismic response of the house for the earthquake used in this article, which is equivalent to the earthquake of September 19, 2017.

The foundation stability evaluation with the alternative procedure of characteristic plans is a simple-to-operate that can help in the design and review of shallow foundations.

a) Plant, cracks path on the surface of the ground. Modified from Google Earth (2017).

b) Condition of cracks A and B and adjacent houses on June 25, 2019.
Figure 14. Condition of houses damaged by soil cracking.

8 ACKNOWLEDGEMENTS

This work was carried out as part of a research sponsored by the Institute for Construction Safety of the Government of Mexico City.

9 REFERENCES

Alberro, J. e Hiriart, G. 1973. Resistencia a largo plazo de las arcillas del Valle de México, *Series del Instituto de Ingeniería*, UNAM, No. 317.

Auvinet, G. 2010. Soil fracturing induced by land subsidence, in Land subsidence, Associated Hazards and the Role of Natural Resources Development, *IAHS Publication*, 339, ISSN 0144-7815, pp. 20-26

Auvinet, G., Méndez, E. and Juárez, M. 2013. Soil fracturing induced by land subsidence in Mexico City, Proceedings, *XVIIIth International Conference on Soil Mechanics and Geotechnical Engineering*, International Society for Soil Mechanics and Geotechnical Engineering, Paris, France.

Auvinet, G., Méndez, E. and Juárez, M. 2015. Evaluation of regional subsidence and soil fracturing in Mexico City Valley, Proceedings, *XVth Pan-American Conference on Soil Mechanics and Geotechnical Engineering*, Buenos Aires, Argentina, November 15-18th 2015.

Auvinet, G., Méndez, E. and Juárez, M. 2017. *El subsuelo de la Ciudad de México, Vol. 3*, Complemento a la Tercera Edición del libro de R.J. Marsal y M. Mazari: Volumen adicional (Vol. 3) sobre avances en el conocimiento del subsuelo 1959-2016, publicado con motivo del 60 aniversario de la fundación del Instituto de Ingeniería, UNAM. ISBN Vol. 3 978-607-02-8198.

Auvinet, G., Juárez, M., Méndez, E., Martínez-Galván, S., Sánchez, J., Hernández, F., Delgado, M., Pineda, A.R. and Román, H. 2019. *Investigación sobre el agrietamiento del suelo en las alcaldías de Iztapalapa, Tláhuac, Xochimilco y Milpa Alta y acompañamiento técnico en la definición e implementación de soluciones para las edificaciones afectadas de dichas demarcaciones*. Universidad Nacional Autónoma de México, Instituto de Ingeniería, Estudio para el Instituto para la Seguridad de las Construcciones (ISC)

Auvinet, G., Juárez, M., Méndez, E., Martínez, S., Hernández, F. and Delgado, M. 2020. *Investigación sobre el agrietamiento del suelo en las alcaldías de Iztapalapa, Tláhuac, Xochimilco y Milpa Alta y acompañamiento técnico en la definición e implementación de soluciones para las edificaciones afectadas de dichas demarcaciones*. Universidad Nacional Autónoma de México, Instituto de Ingeniería, Estudio para el Instituto para la Seguridad de las Construcciones (ISC).

Auvinet, G., Juárez, M., Méndez, E., Hernández, F. and Pérez M. 2021, Evaluación del mecanismo de agrietamiento del suelo en el suroriente de la Ciudad de México mediante exploración profunda, Memoria, *XXXa Reunión Nacional de Ingeniería Geotécnica*, CDMX, México, Sociedad Mexicana de Ingeniería Geotécnica (SMIG), publicación digital, marzo, pp. 1053-1064.

CFE 2015. *Manual de Diseño de Obras Civiles – Diseño por Sismo*, México, (Prodisis software).

Bowles, J. E., 1997. *Foundation analysis and design*. 5th Edition, McGraw-Hill, p1207.

GCDMX 2017a. *Norma Técnica Complementaria sobre Criterios y Acciones para el Diseño Estructural de las Edificaciones*.

GCDMX 2017b. *Norma Técnica Complementaria para Diseño y Construcción de Cimentaciones*.

GCDMX 2017c. *Norma Técnica Complementaria para Diseño y Construcción de Estructuras de Mampostería*.

GCDMX 2017d. *Norma Técnica Complementaria para Diseño por Sismo*.

Gourvenec, S. 2007. Shape effects on the capacity of rectangular footings under general loading, *Geotechnique*, 57, No. 8, 637–646 doi:10.1680/geot.2007.57.8.637.

Martínez-Galván, S. A., Auvinet, G. and Juárez, M. 2021. Análisis numérico del comportamiento sísmico del subsuelo en presencia de grietas, Memoria, *XXXa Reunión Nacional de Ingeniería Geotécnica*, CDMX, México, Sociedad Mexicana de Ingeniería Geotécnica (SMIG), publicado en digital, marzo, pp. 1033-1040.

Méndez-Sánchez, E., Auvinet-Guichard G., Sánchez Palma J. L., García Salazar J. A. and Díaz Soteno J. A. 2012. Agrietamiento del suelo en los tres principales valles del altiplano mexicano, Memoria, *XXVIa Reunión Nacional de Mecánica de Suelos e Ingeniería Geotécnica*, Sociedad Mexicana de Ingeniería Geotécnica, 14-16 noviembre de 2012, Cancún, Quintana Roo, México.

Plaxis bv., 2020. *Manual de usuario Plaxis-3D*. Plaxis bv, Netherlands, Service Nr: 2-1312457.

Salençon, J. and Pecker, A. 1995-a. Ultimate bearing capacity of shallow foundations under inclined and eccentric loads. Part I. Purely Cohesive Soil, *European Journal of Mechanics, A/Solids* 14(3), 349-375

Salençon, J. and Pecker, A. 1995-b. Ultimate bearing capacity of shallow foundations under inclined and eccentric loads. Part II. Purely Cohesive Soil without tensile strength, *European Journal of Mechanics, A/Solids* 14(3), 377-396

Velasco, E., Auvinet, G., Juárez, M. and Martínez-Galván, S. 2022. Análisis de la vulnerabilidad de las cimentaciones de edificaciones en la Ciudad de México, Memoria, *XXXIa Reunión Nacional de Ingeniería Geotécnica*, Guadalajara, noviembre.